Transit observations and hydrogen and ENA–cloud modelling as a tool for exoplanet magnetic and plasma environment characterization

K. G. Kislyakova (1), M. L. Khodachenko (2), H. Lammer (2), I. Alexeev (3), E. Belenkaya (3), J.-M. Griessmeier (4), M. Holmstroem (5), Yu. N. Kulikov (6), V. I. Shematovich (7), D. Bisikalo (7)

1 N. I. Lobachevsky State University, University of Nizhnij Novgorod, 603950 Nizhnij Novgorod, Russian Federation
2 Space Research Institute, Austrian Academy of Sciences, A-8042 Graz, Austria
3 Skobelitsyn Institute of Nuclear Physics, Lomonosov Moscow State University, 119992 Moscow, Russian Federation
4 Laboratoire de Physique et Chimie de l'Environnement et de l'Espace, CNRS, Avenue de la Recherche Scientifique, 45071 Orlűans, France
5 Swedish Institute of Space Physics, Box 812, SE-98128 Kiruna, Sweden
6 Polar Geophysical Institute, Russian Academy of Sciences, 183010 Murmansk, Russian Federation
7 Institute of Astronomy, Russian Academy of Sciences, Moscow, Russian Federation
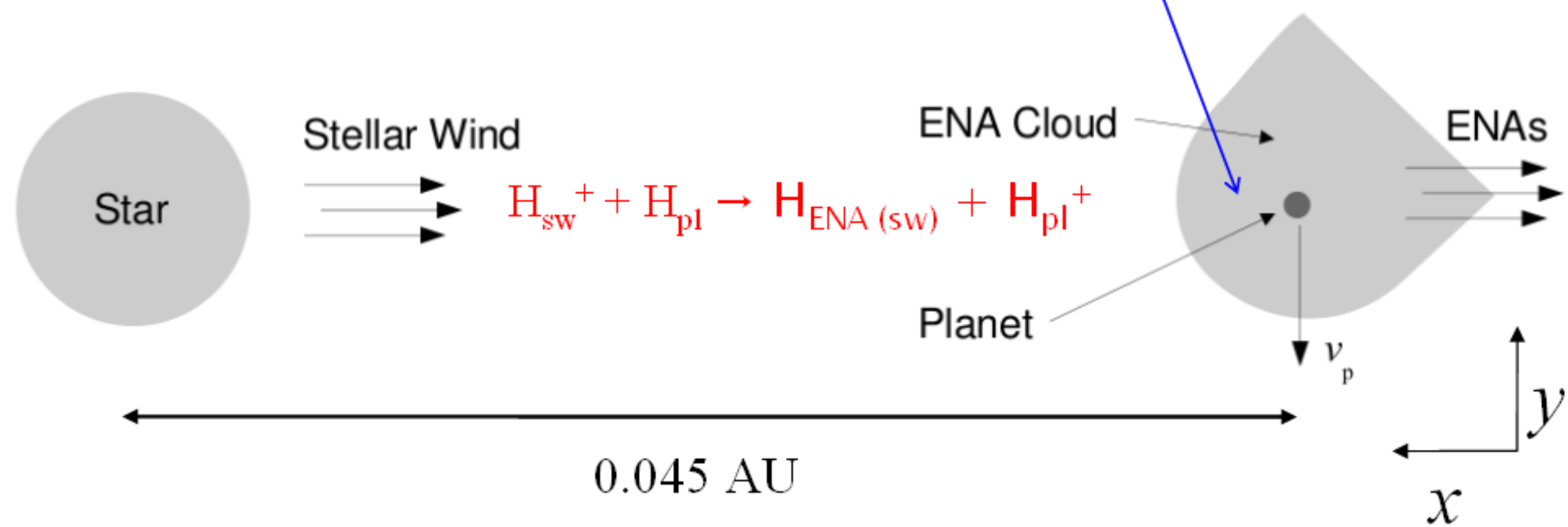
HD 209458b

Fig.1: ENAs production.

Energetic neutral atoms (ENAs) are produced wherever energetic ions meet a neutral atmosphere, and solar wind ENAs have been observed at every planet in the Solar System where ENA instrumentation has been available — at Earth[1], at Mars[2], and at Venus[3]. Absorption features can be explained very well by ENA production. Without ENA production in the model, none of the spectral features are present.
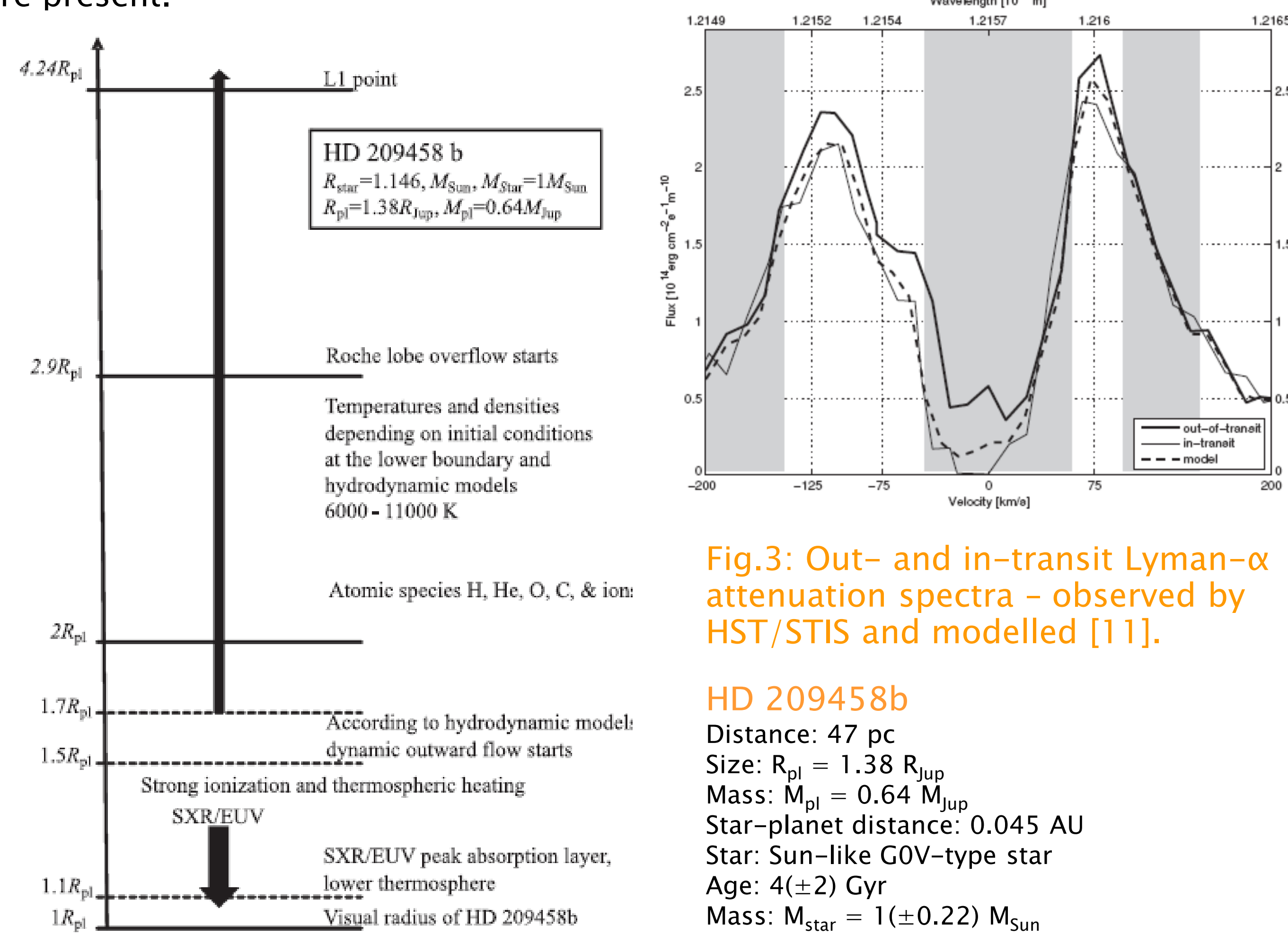

Fig.3: Out- and in-transit Lyman–α attenuation spectra – observed by HST/STIS and modelled [11].

HD 209458b
Distance: 47 pc
Size: R_{pl} = 1.38 R_{Jup}
Mass: M_{pl} = 0.64 M_{Jup}
Star-planet distance: 0.045 AU
Star: Sun-like G0V–type star
Age: 4(±2) Gyr
Mass: M_{star} = 1(±0.22) M_{Sun}

Fig.2: upper atmosphere structure of HD 209458b.

HD 209458b is one of the best studied Jupiter-type exoplanets for which several transits in front of its Sun–like host star were observed by Charbonneau et al. (2000) and Henry et al. (2000). Later observations with the Hubble Space Telescope (HST) show absorption in the stellar Lyman–α line at 1215.67 Å during transits, which revealed that the planets thermosphere is most likely not under hydrostatic conditions and expands up or even beyond the Roche lobe. Fig.2 illustrates the possible upper atmosphere structure of HD 209458b according to hydrodynamic and empirical models [4–9]. Fig. 3 shows the out- and in-transit Lyman–α attenuation spectra – observed by HST/STIS and modelled with produced ENAs by [11].
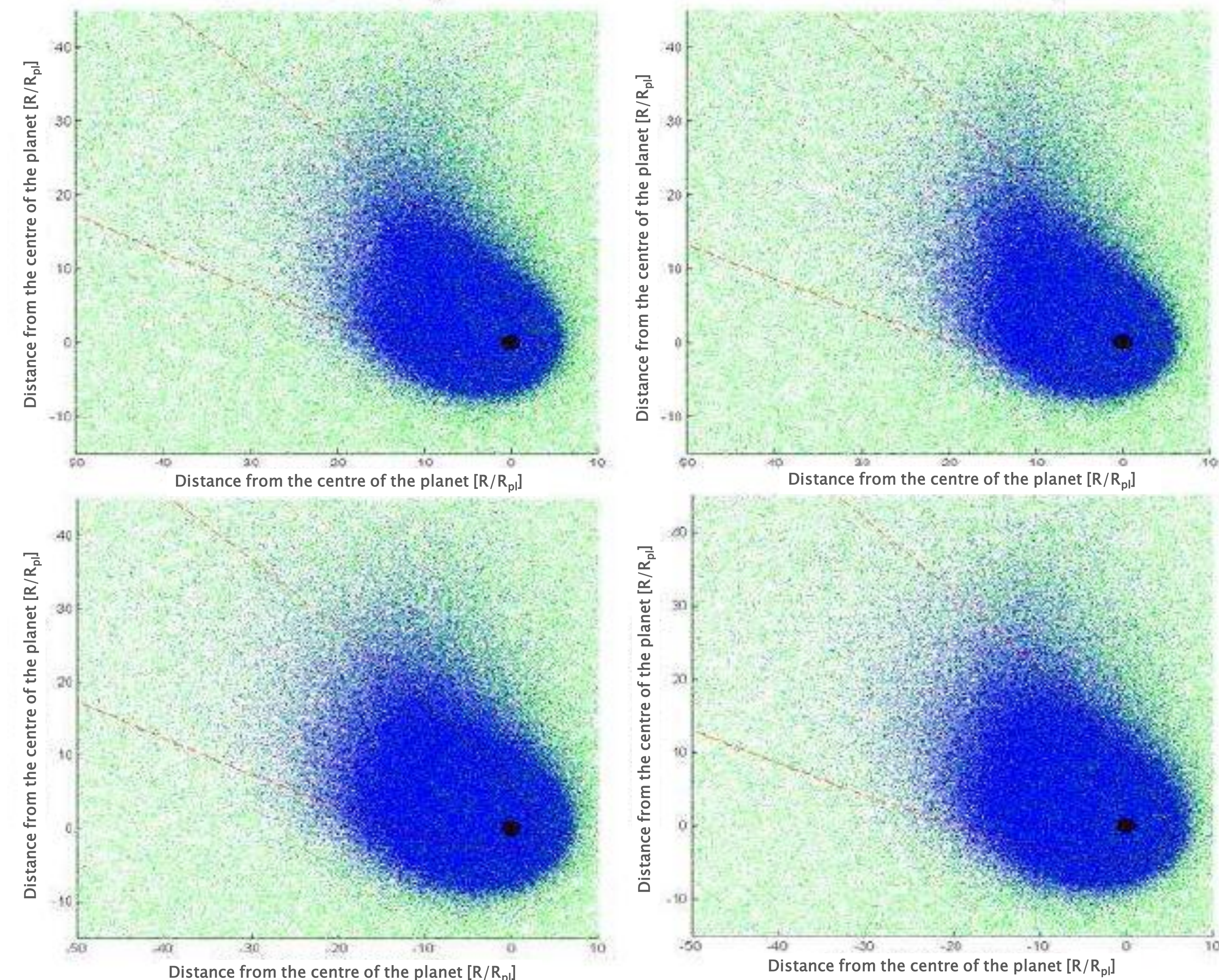

Fig. 6: Planetary hydrogen and ENA-clouds around HD 209458b for exobase temperatures of 8000 K and 11000 K and magnetopause obstacles at about 3.6 R_{pl} (weaker magentic field: left panel) and 5.5 R_{pl} (stronger magnetic field: right panel).
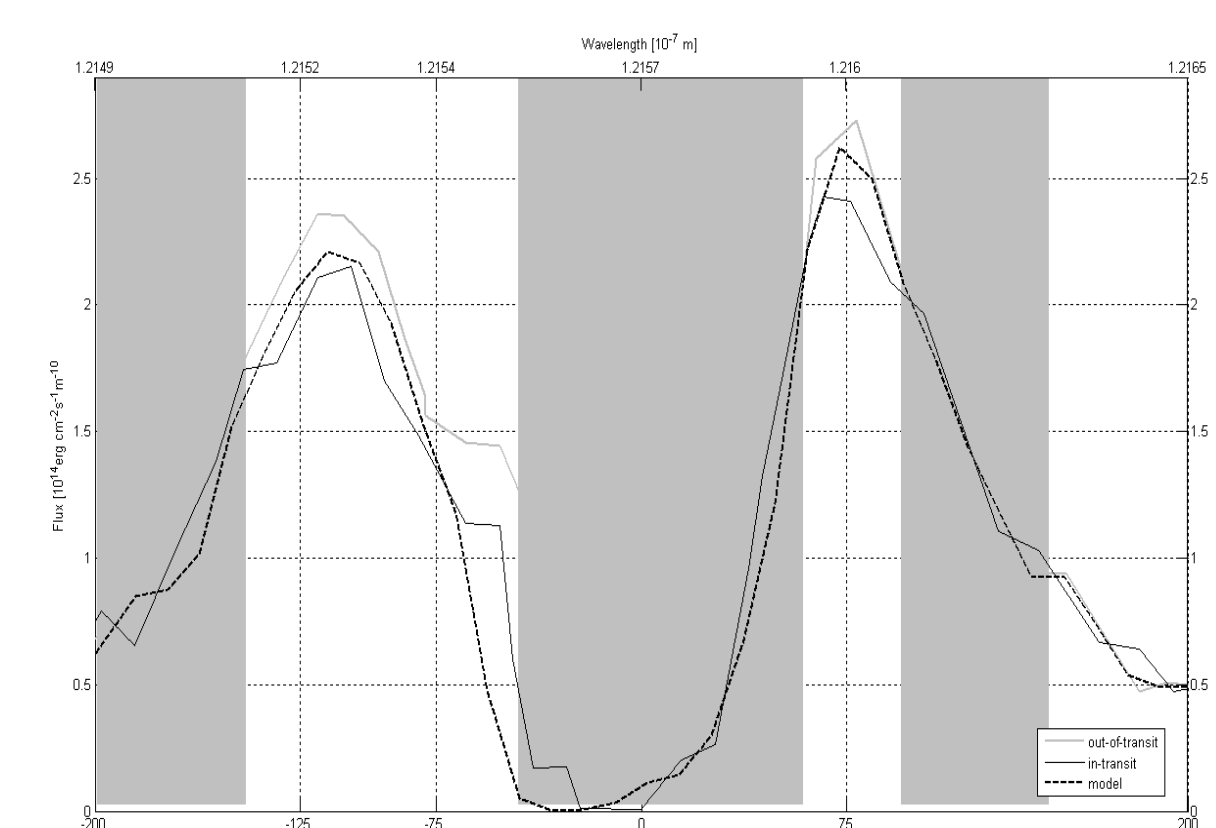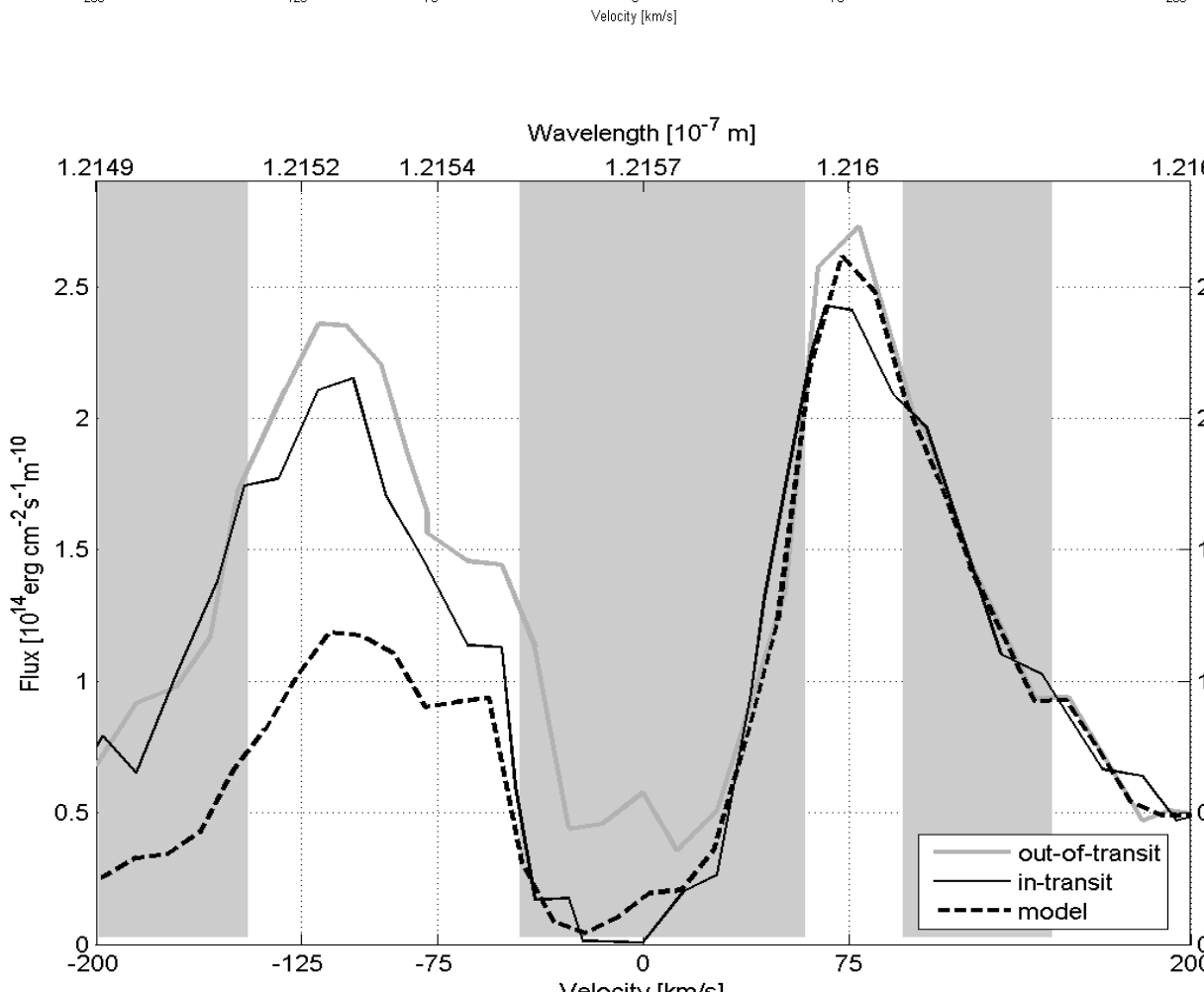

Fig. 8 upper panel: Comparison of the modelled Lyman–α profile (ENA) with the HST observation by including the modelled PPM configuration and a dynamo field of about 10 % of the field strength of Jupiter.

Lower panel: Similar model run with a weaker dynamo field and an magentic obstacle which is closer at the planet.
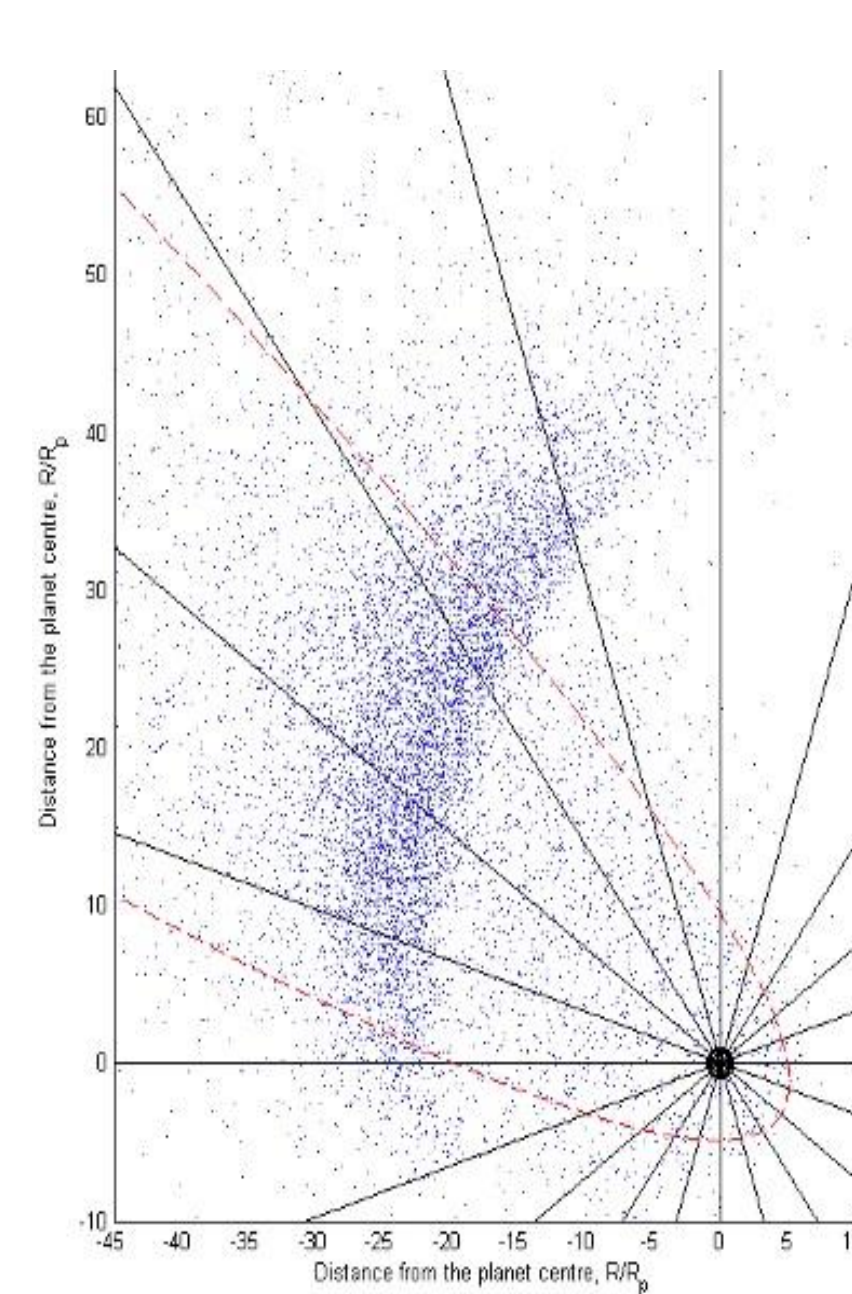

Fig.7: ENA cloud around HD 209458b. Dotted line shows the magnetic obstacle projection. Only atoms with the velocities greater then 50 km/s are plotted.

Abstract: During the previous years spacecraft observations of so-called Energetic Neutral Atoms (ENAs) have become an important remote-sensing technique in planetary science for analyzing the solar wind plasma flow around the upper atmospheric environments of Solar System bodies. ENAs are produced whenever solar- or stellar wind protons interact via charge exchange with a neutral particle from a planetary atmosphere so that their signals constrain both, ion distributions and neutral gas densities. We discuss how ENA-observations and data interpretations of attenuation and velocity spectra obtained from transiting hydrogen-rich exoplanets such as HD 209458b can be used for the study of the upper atmosphere structure, the planet's magnetosphere and information on stellar wind properties. Finally, we discuss how future hydrogen cloud observations around exoplanets by space observatories like the Russia-led World Space Observatory–UV (WSO-UV) together with ESAs PLATO mission can be used for the test of magnetic dynamo hypotheses of exosolar gas giants.

PMM – paraboloid magnetosphere model

Because the production of ENAs around "hot Jupiters" such as HD 209458b depends on the planetary obstacle to the stellar wind it is important to calculate a sub-stellar magnetopause stand-off distance which corresponds to a realistic magnetospheric shape. In the studies of Holmström et al. [10] and Ekenbäck et al. [11] a simple cone shaped magnetosphere obstacle was assumed. Recently, Khodachenko et al. [12] applied a paraboloid magnetosphere model (PMM) for the study of "hot Jupiter" magnetospheres and found that currents which flow inside a magnetodisk induce a strong magnetic field which contributes essentially to the intrinsic dynamo field strength and magnetosphere topology.

Because this additional magnetic field and its influence to the magnetosphere and magnetopause topology was neglected in previous ENA studies in [10] and [11] we calculated the magnetodisk field and the corresponding magnetosphere configuration for this study. The main contributors to the magnetic field in the PMM model can be summarized as [12]:
· a planetary intrinsic magnetic dipole field (corresponding to dynamo hypotheses),
· a magnetic field of a current disc around the planet,
· a magnetopause current that confines the dipole and magnetodisk fields inside the magnetopause,
· dawn-to-dusk directed cross-tail currents and their closure currents on the magnetopause,
· the IMF, that partially penetrates into the magnetosphere as a result of reconnection with the planetary magnetic field.

Paraboloid Magnetospheric Model (PMM) for "Hot Jupiters"
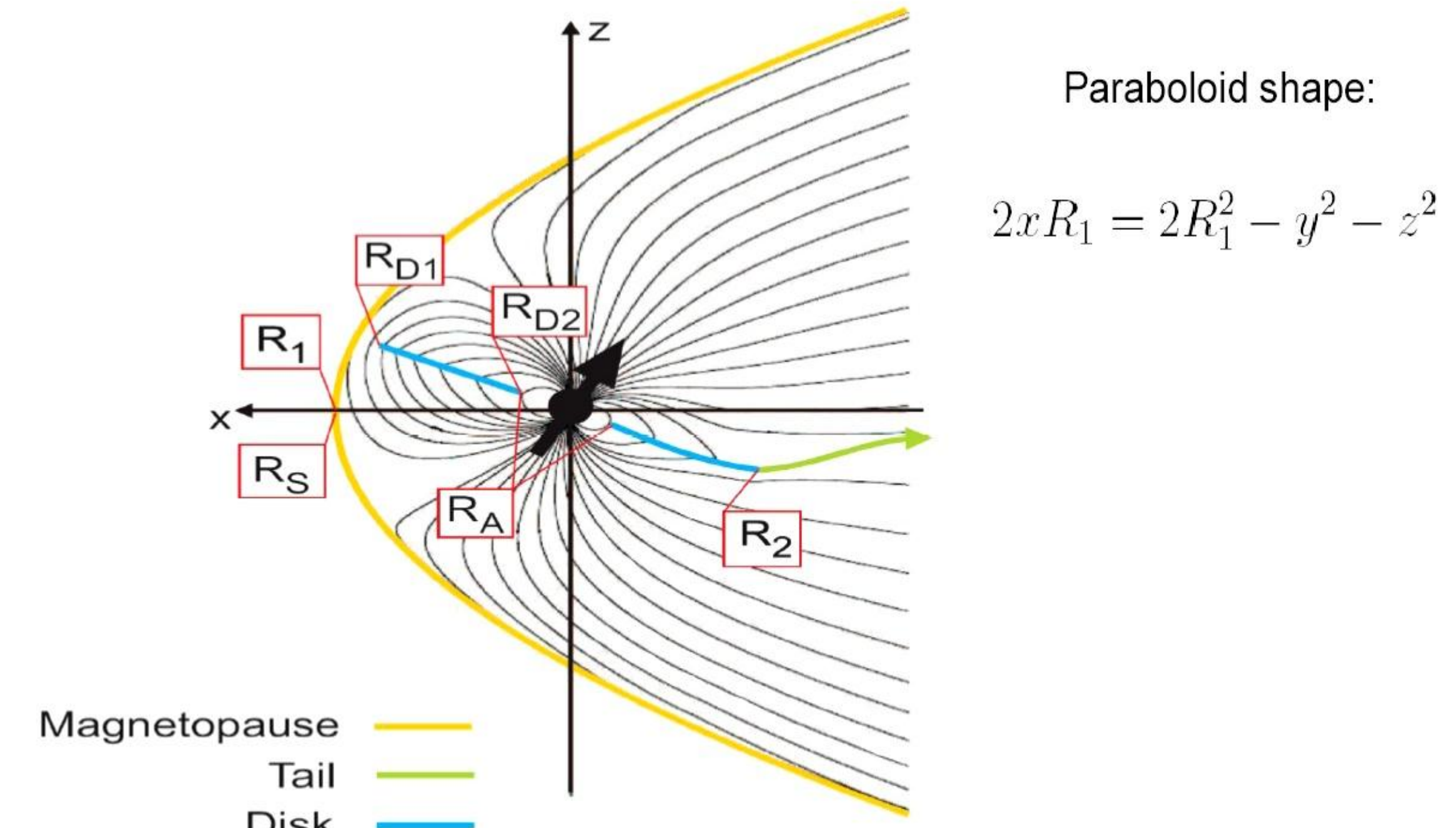
♦ Schematic view of PMM elements:

Paraboloid shape:
$$2xR_1 = 2R_1^2 - y^2 - z^2$$

Fig.4. PMM.

Formation of a magnetodisk

– "sling" model:
dipole mag. field can drive plasma in co-rotation regime only inside "Alfvenic surface" ($r < R_A$); → Centrifugal escape of plasma

– "mass-loss driven" models: → Hydrodynamic upward flow of expanting plasma

(a) Fully ionized plasma outflow – similarity with heliospheric current sheet (disk)

(b) Partially ionized material outflow – background magnetic field (dipole), charge separation electric field, ambipolar diffusion, azimuth. Hall current in equatorial plane
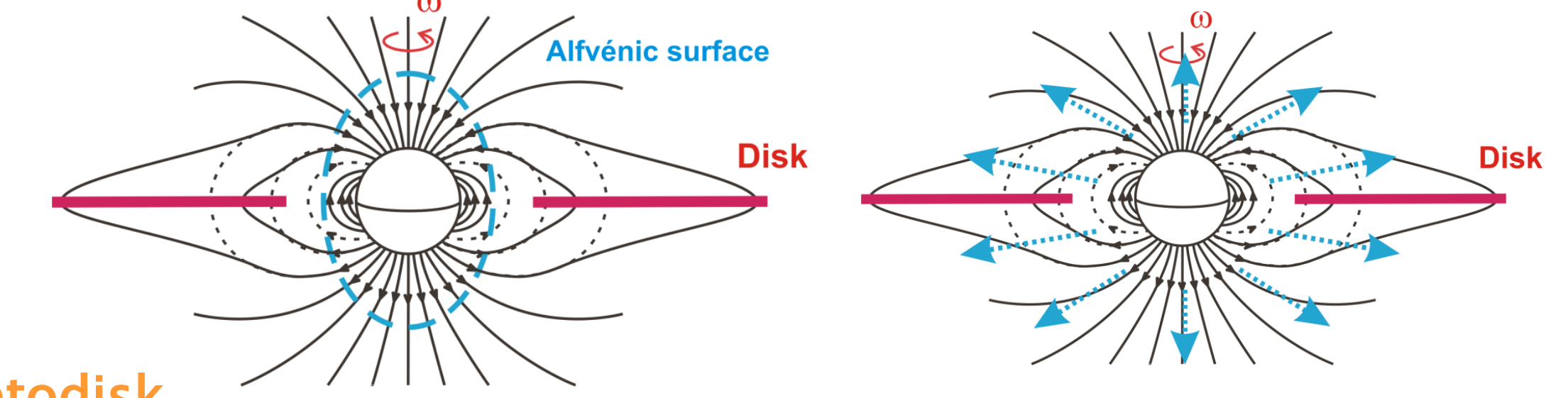

Fig. 5: Sling model and mass loss model.

Magnetic field structure in PMM with magnetodisk

– $r < R_A$: magnetic field of dipole ($\sim R^{-3}$)

– $r > R_A$: conservation of magnetic flux reconnected across the disc
⇒ magnetic field of the disk (and current density)
$$\mathbf{B}(r, z = 0) = B_\theta(r)\theta_0 = B_{d0}r_p^3/r^3\,\theta_0$$

Determination of sub-stellar magnetopause distance:
pressure balance condition $\mathbf{B}(r, z \sim 0) = B_r(r)\,\mathbf{r_0} = B_{d0}r_p^3/(R_A r^2)\,\mathbf{r_0}$ $\sim R^{-2}$

Decrease of R_A causes increase of R_S $\quad \rho_{sw}\tilde{v}_{sw}^2 = \dfrac{\kappa^2(B_{ds} + B_{MDs})}{2\mu_0} + p_{mp}$ $\quad R_s \sim \dfrac{B_{d0}^{1/2} r_p^{3/2}}{(2\mu_0 p_{sw})^{1/4} R_A^{1/2}}(1 + \kappa^2)^{1/4}$

A model of ENA production around HD 209458b

Here we model the ENA production by an advanced particle code that includes stellar wind protons and atomic hydrogen. Charge exchange between stellar wind protons and exospheric hydrogen takes place outside a conic obstacle that represents the magnetosphere of the planet with a plasma disc, which is calculated by using the PMM model. The resulting planetary hydrogen and ENA clouds are shown in Fig. 6. Fig. 7 shows only neutral H-atoms with velocities greater than 50 km/s (ENAs). The dashed lines represent the obstacles. Fig. 8 illustrates a comparison of the modelled Lyman–α profiles with the observed one. The black solid line represents the observations of the Lyman–α flux during the transit, the gray solid line corresponds to the out-of-transit observations, while the dashed line illustrates the results of the numerical modeling. The "GEO" region is the region of the geocoronal emission at low velocities is excluded. These spectra which are shown are still preliminary and correspond to upper atmosphere temperatures of about 8000-11000 K. The lower panel in Fig. 8 shows the ENA production when the obstacle is closer to the planet and the stellar wind density is strong. Simulation are in progress which will choose stellar wind densities and velocities as well as PPM magnetosphere obstacles which should yield the best absorbtion.

WSO-UV

The WSO-UV incorporates a primary mirror of 1.7m diameter (i.e. with just half the collecting area of HST), but taking advantage of the modern technology for astronomical instrumentation, and a high altitude, high observational efficiency orbit, the WSO-UV will provide UV-optical astronomical data quantitatively and qualitatively comparable to the exceptional data base collected by HAST. WSO-UV follow-up observations of exoplanets discovered by PLATO should enhance our understanding related to the aeronomy of exoplanets, plasma interatcion and magentospheric environments [13].

Telescope: T-170M, *Russia.*
1.7 m diameter, primary λ range 110 – 340 nm,
Spectrographs: *Germany, Russia*
UVES, VUVES, R ≈ 5–6 x 10⁴;
LSS, R ≈ 2500
Imaging: FCU, *Spain*
FUV channel optimised for Lyα mapping of faint targets survey channel. Beam splitter:
FUV 120–200 nm, UVO 200–650 nm
Platform: Navigator, *Russia*
Orbit: geosynchronous one with i=51.6º is considered as working orbit
Launcher, launch: "ZENIT 2SB", 2014, *Russia*
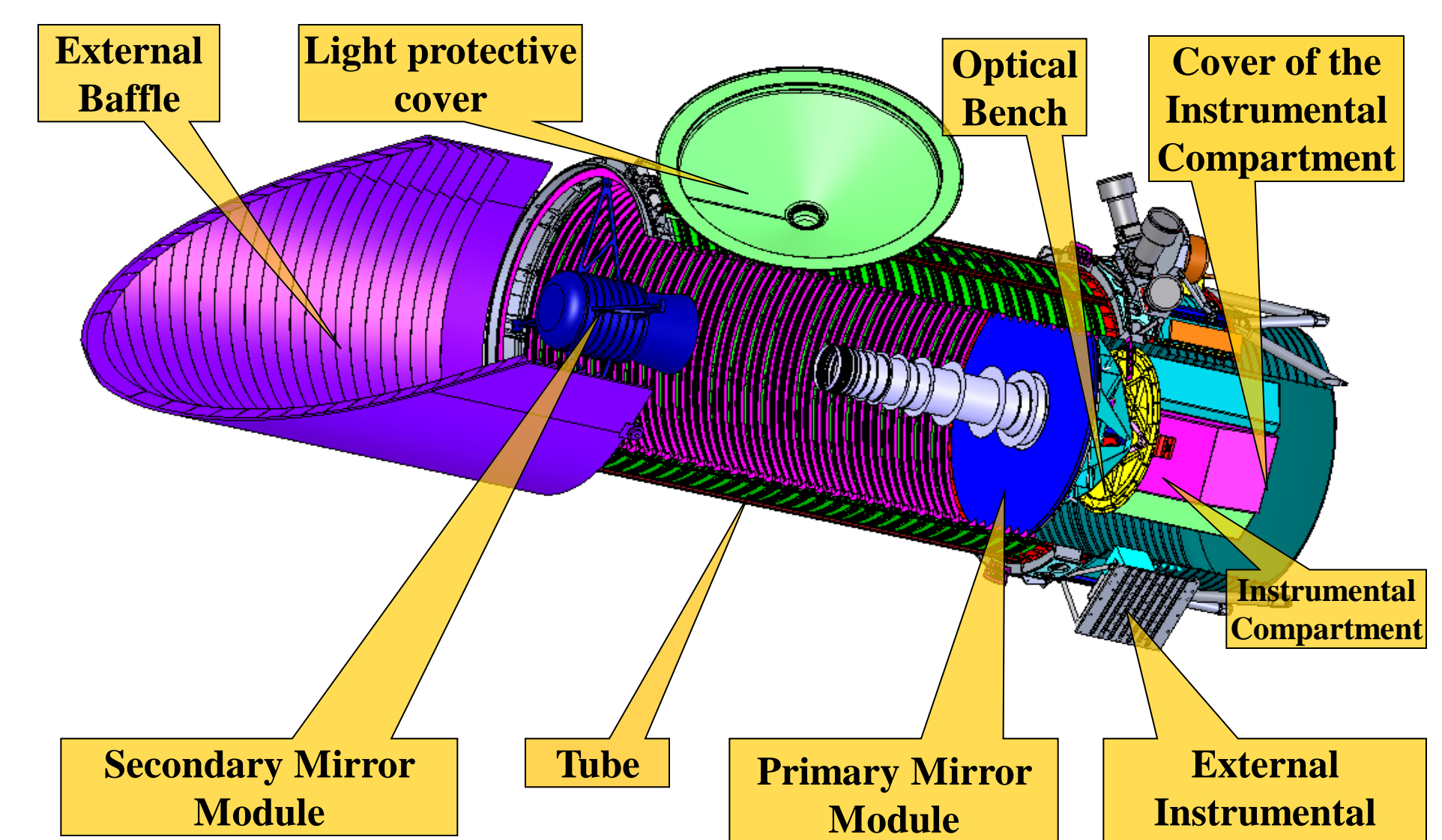**Ground segment**: *Russia, Spain*

Fig. 5: Structure of the WSO-UV T170 M telescope.

References
[1] Collier, M. R., et al.: JGR 106(A11), 24893 (2001)
[2] Futaana, Y., et al.: Icarus, 182(2), 413 (2006)
[3] Galli, A., et al.: Planet. Space Sci., (2007)
[4] Charbonneau, D., et al.: Astrophys. J. 529, L45 (2000)
[5] Henry, G. W., et al., ApJ, 529, L41 (2000)
[6] Yelle, R.V.: Icarus 170, 167 (2004)
[7] Garcia Munoz, A.: Planet. Space Sci., 55, 1426 (2007)
[8] Koskinen, T.T., et al.: ApJ, 723, 116 (2010a)
[9] Koskinen, T.T., et al.: ApJ, 722, 178 (2010b)
[10] Holmström, M., et al.: Nature 451, 970 (2008)
[11] Ekenbäck, A., et al.: 2010, ApJ, 709, 670 (2010)
[12] Khodachenko, M.L., et al. ApJ, submitted (2011)
[13] Shustov, B., et al.: Astrophys. Space Sci. 320, 187 (2009)